CO Binding onto Heterometals of [MoSM] (M = Fe, Co, Ni) Cubes

AUTHOR(S):

Tanifuji, Kazuki; Sakai, Yuta; Matsuoka, Yuto; Tada, Mizuki; Sameera, W. M. C.; Ohki, Yasuhiro

CITATION:

Tanifuji, Kazuki ...[et al]. CO Binding onto Heterometals of [MoSM] (M = Fe, Co, Ni) Cubes. Bulletin of the Chemical Society of Japan 2022, 95(8): 1190-1195

ISSUE DATE:

2022-08

URL:

http://hdl.handle.net/2433/276082

CO Binding onto Heterometals of [Mo_3S_4M] (M = Fe, Co, Ni) Cubes

Kazuki Tanifuji,[1] Yuta Sakai,[1,2] Yuto Matsuoka,[1] Mizuki Tada,[2] W. M. C. Sameera,[3,4] and Yasuhiro Ohki[1]

[1]*Institute for Chemical Research, Kyoto-University, Gokasho, Uji 611-0011, Japan*

[2]*Department of Chemistry, Graduate School of Science and Research Center for Materials Science, Nagoya University, Furo-cho, Chikusa-ku, Nagoya 464-8602, Japan*

[3]Institute for Low Temperature Science, Hokkaido University, Sapporo 060-0819, Japan

[4] Department of Chemistry, University of Colombo, Colombo 00300, Sri Lanka

E-mail: < ohki@scl.kyoto-u.ac.jp >

Yasuhiro Ohki
Yasuhiro Ohki received his Ph.D. from Tokyo Institute of Technology in 2002. He joined Department of Chemistry at Nagoya University as an assistant professor in 2000, and was promoted to an associate professor in 2008. Since 2021, he has been a professor at Institute for Chemical Research, Kyoto University. His research interests include organometallic chemistry and bioinorganic chemistry with an emphasis on developing new synthetic methodologies for inorganic molecules.

Abstract

We have previously shown that cyclopentadienyl (Cp^R)-supported [Mo_3S_4] platforms capture and stabilize halides of hetero-metals (M) under reducing conditions to give [Mo_3S_4M] cubes. Here we report Co and Ni variants with Cp^{XL} ligands (Cp^{XL} = $C_5Me_4SiEt_3$) and CO binding to the [Mo_3S_4M] clusters (M = Fe, Co, Ni). Properties of the isolated CO-bound [Mo_3S_4M] cubes were investigated by X-ray diffraction, IR, and electrochemical analyses. Density functional theory (DFT) calculations were performed for the isolated CO-bound clusters to evaluate M-CO interactions. These analyses constitute foundations to develop bio-mimetic molecular catalysts for the direct conversion of CO and/or CO_2 into hydrocarbons, which can contribute to the reduction of carbon emissions.

Keywords: Metal-sulfur clusters, Carbon monoxide, Iron-group metals

1. Introduction

Transition metal-sulfur (M-S) clusters, which consist of multiple metals and sulfur atoms, play various roles as metallocofactors of proteins. Heterometallic M-S cofactors are uniquely found to catalyze the reduction of small inert molecules: for instance, a Mo-Fe-S-C cluster in nitrogenase ([(*R*-homocitrate)$MoFe_7S_9C$], FeMoco or M-cluster) is known to transform N_2 into NH_3,[1] and a Ni-Fe-S cluster in CO-dehydrogenase ([$NiFe_4S_4$], C-cluster) mediates the conversion of CO_2 to CO.[2] Synthetic M-S clusters have gained attention as an approach to reproduce such natural functions as cofactor models. Nevertheless, the reaction chemistry of this class of compounds is still under development, particularly regarding small-molecule activation.[3] Our previous studies corroborated that a heterometallic-cubane [Mo_3S_4M] (M = transition metals) is suitable to perform such reactivity studies, as demonstrated by the activation of N_2.[4] Precursors for the [Mo_3S_4M] cubes are cyclopentadienyl (Cp^R)-supported [Mo_3S_4] platforms, in which three μ-sulfides firmly hold one M atom. Steric protection around M imposed by the Cp^R ligands on Mo is also vital to prevent undesirable decomposition or aggregation of the resultant [Mo_3S_4M] cubes.[5] Related protection approaches have been helpful for isolating some cubic M-S clusters with reactive fragments or N_2.[6] In line with the chemistry of the [Mo_3S_4M] clusters, we report herein the synthesis of Co and Ni variants of the [Mo_3S_4M] clusters, [$Cp^{XL}{}_3Mo_3S_4MCl$] (M = Co (**1a**), Ni (**1b**); Cp^{XL} = $C_5Me_4SiEt_3$) that are analogous to the known [Mo_3S_4Fe] cluster, [$Cp^{XL}{}_3Mo_3S_4FeCl$] (**1c**).[5b] CO-binding behaviors of clusters **1a-c** were tested and discussed based on experimental and theoretical results and comparison with recently reported [$Cp^{XL}{}_3Mo_3S_4Fe(CO)$] (**3**).[7] These results give a fundamental understanding of M-CO interactions in metal-sulfur clusters with *iron triad* metals (Fe, Co, Ni). This study will also be beneficial in developing molecular catalysts for the direct conversion of CO_2 into fuels, as CO represents a key intermediate in this multi-step reaction. We have previously demonstrated such catalytic carbon-fixation reactions with various synthetic metal-sulfur clusters;[8] however, no mechanistic insight regarding binding behaviors of substrates has been provided thus far.

2. Results and Discussion

Synthesis of CO-bound [Mo_3S_4M] clusters. The [Mo_3S_4M]

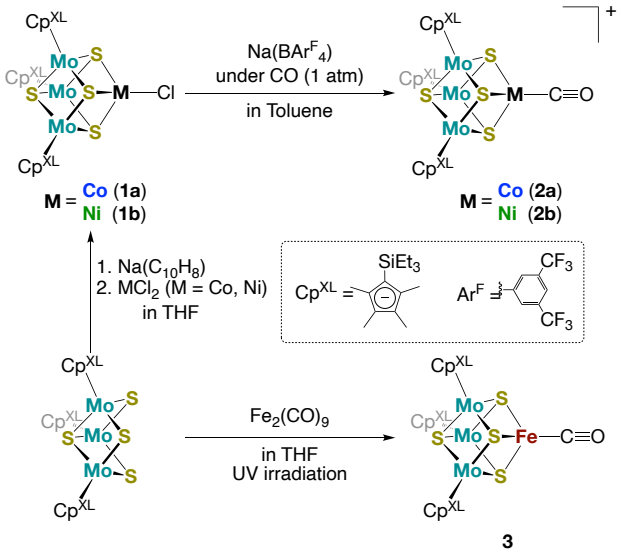

Scheme 1. Synthesis of [$Cp^{XL}{}_3Mo_3S_4MCl$] (M = Co (**1a**), Ni (**1b**)), [$Cp^{XL}{}_3Mo_3S_4M(CO)$] (M = Co (**2a**), Ni (**2b**)), and [$Cp^{XL}{}_3Mo_3S_4Fe(CO)$] (**3**). Cp^{XL} = $C_5Me_4SiEt_3$.

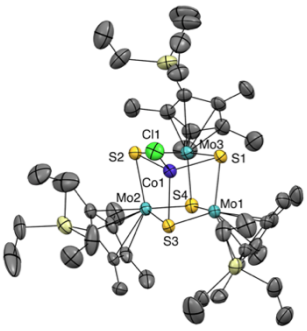

Figure 1. Crystal structure of $[Cp^{XL}{}_3Mo_3S_4CoCl]$ (**1a**) with thermal ellipsoids displayed at 50% probability level. The unit cell contains two independent molecules of **1a**. These molecules label their cobalt atoms as Co1 and Co2. Selected bond distances (Å): Co1-Mo1, 2.8599(4); Co1-Mo2, 2.7827(5); Co1-Mo3, 2.7665(6); Co1-S1, 2.2159(9); Co1-S2, 2.2137(9); Co1-S3, 2.218(9); Co2-Mo4, 2.7626(5); Co2-Mo5, 2.7793(6); Co2-Mo6, 2.7642(6); Co2-S5, 2.2091(10); Co2-S6, 2.2224(10); Co2-S7, 2.2140(10).

cubes (M = Co and Ni) with bulky Cp^{XL} ligands on Mo atoms and chloride on M were prepared analogously to the synthesis of $[Cp^{XL}{}_3Mo_3S_4FeCl]$.[5b] Sequential treatment of $Cp^{XL}{}_3Mo_3S_4$ with $Na(C_{10}H_8)$ and $CoCl_2$ or $NiCl_2$(DME) (DME = 1,2-dimethoxyethane) gave rise to the corresponding clusters $[Cp^{XL}{}_3Mo_3S_4MCl]$ (M = Co (**1a**), Ni (**1b**)) in reasonable yields as crystals (43 and 49%, respectively, Scheme 1, left). A related synthetic protocol is known for the preparation of $[Fe_3S_4M]$ cubes. Holm and coworkers used a linear-type $[Fe_3S_4]$ cluster bearing bulky mesityl thiolates ($^-$SMes), which was treated with Co and Ni sources to give $[MFe_3S_4(SMes)_4]^{2-}$ (M = Co, Ni).[9] The molecular structures of **1a** and **1b** were determined by X-ray crystallographic analysis, as shown in Figures 1 and S12. As was found with the Fe analog, the incorporated heterometal M is in a distorted tetrahedral geometry with three sulfides and a potentially labile Cl atom. The $SiEt_3$ groups of Cp^{XL} ligands are located around the M-Cl moiety. The M-Mo, M-S, and Mo-S distances of **1a** and **1b** are comparable to the known $[Mo_3S_4Co]$[5a, 10] and $[Mo_3S_4Ni]$[10e, 11] clusters, suggesting that the steric and electronic properties of Cp^R-ligands on Mo do not affect the cubic structures significantly. Cyclic voltammetry measurement of **1a** in THF revealed reversible $[Mo_3S_4Co]^{5+/4+}$ and $[Mo_3S_4Co]^{4+/3+}$ couples at –0.70 and –1.70 V vs. Fc/Fc^+ (Fc = Cp_2Fe), whereas **1b** displayed only a $[Mo_3S_4Ni]^{5+/4+}$ couple at –0.22 V (Figures S9 and S11).

Abstraction of the chloride from clusters **1a** and **1b** by $NaBAr^F{}_4$ (Ar^F = 3,5-$(CF_3)_2C_6H_3$) under a CO atmosphere (1 atm) in toluene resulted in the formation of the cationic CO-clusters (Scheme 1), $[Cp^{XL}{}_3Mo_3S_4Co(CO)](BAr^F{}_4)$ (**2a**·$(BAr^F{}_4)$) and $[Cp^{XL}{}_3Mo_3S_4Ni(CO)](BAr^F{}_4)$ (**2b**·$(BAr^F{}_4)$), of which CO stretches were observed at 1992 cm^{-1} and 2039 cm^{-1} in the infrared (IR) spectra (Figure 2). These Cl-to-CO

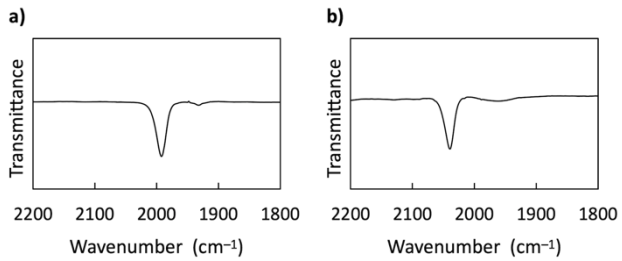

Figure 2. IR spectra of a) $[Cp^{XL}{}_3Mo_3S_4Co(CO)]^+$ (**2a**) and b) $[Cp^{XL}{}_3Mo_3S_4Ni(CO)]^+$ (**2b**) in THF, showing their CO stretching bands.

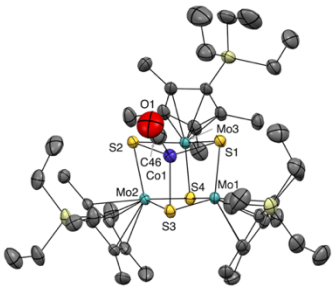

Figure 3. Structure of the cationic part of **2a** with thermal ellipsoids displayed at 50% probability level. Selected bond distances (Å): Co1-Mo1, 2.7396(4); Co1-Mo2, 2.7397(4); Co1-Mo3, 2.7436(4); Co1-S1, 2.2082(7); Co1-S2, 2.2050(6); Co1-S3, 2.2023(6); Co1-C46, 1.834(4); C46-O1, 0.992(4).

substitution reactions were completed within 30 min at room temperature, which was monitored by ^{1}H NMR in C_6D_6. The products were isolated as black crystals in 49 and 65% yields, respectively, and characterized based on the NMR spectra, mass spectrometry, and elemental analysis. Retention of the $[Mo_3S_4M]$ (M = Co or Ni) core in **2a** and **2b** was confirmed by their crystal structures (Figures 3 and S13), which exhibit cubes with one terminal M-CO moiety and accompanying $BAr^F{}_4$ counter-anion (see more details in Supporting Information).

In contrast to the facile and clean formation of **2a** and **b**, an analogous reaction of the Fe-variant $[Cp^{XL}{}_3Mo_3S_4FeCl]$ (**1c**) with $NaBAr^F{}_4$ under CO afforded a complex mixture of unidentifiable products. An IR spectrum of the dried residue of this reaction did not display any diagnostic CO stretching band, indicating the absence of metal-bound CO in the reaction product(s). On the other hand, a direct incorporation of Fe-CO moiety to the incomplete-cubane $[Mo_3S_4]$ platform was successful and led to the formation of $[Cp^{XL}{}_3Mo_3S_4Fe(CO)]$ (**3**) (Scheme 1, bottom).[7] Cluster **3** displayed a CO stretching frequency at 1877 cm^{-1}, which is significantly lower than the values for **2a** and **2b**. While it is reasonable that the more reduced cluster (**3** in $[Mo_3S_4Fe]^{3+}$ state) exhibits stronger back donation than more oxidized species (**2a** and **2b** in $[Mo_3S_4M]^{4+}$ states), these distinct differences over 100 cm^{-1} suggest effective interactions between Fe *d* orbitals and CO π^* orbitals as further theoretical analyses given below.

Crystal Structures of CO-bound clusters $[Cp^{XL}{}_3Mo_3S_4M(CO)]^+$ (M = Co (2a), Ni(2b); Cp^{XL} = $C_5Me_4SiEt_3$). Each of the CO-bound clusters ($[Cp^{XL}{}_3Mo_3S_4Co(CO)]^+$ (**2a**) and $[Cp^{XL}{}_3Mo_3S_4Ni(CO)]^+$ (**2b**)) was structurally determined as the pair of $[Mo_3S_4M]$ cation with a terminal CO ligand and a $BAr^F{}_4$ anion. Even though the charge is different between the Cl- and CO-bound forms, the bond distances within the cubes are comparable. The Ni series (**1b** and **2b**) reveals indistinguishable mean Ni-S and Ni-Mo distances, 2.214(4) Å for **1b** vs. 2.219(11) Å for **2b** (Ni-S), and 2.728(5) Å for **1b** and 2.749(16) Å for **2b** (Ni-Mo). In contrast, the Co series (**1a** and **2a**) exhibits only slight shortening of the mean Co-S and Co-Mo distances upon CO binding: *e.g.*, 2.216(5) Å for **1a** vs. 2.2052(2) Å for **2a** (Co-S) and 2.768(10) Å for **1a** vs. 2.741(2) Å for **2a** (Co-Mo).

Several CO-bound $[Mo_3S_4Co]$ clusters have been structurally characterized[10a-c] as $[Mo_3S_4Co]^{3+}$ species that are in the one-electron reduced state relative to **2a**. As expected from the lower oxidation state, their CO stretching frequencies (1903 to 1923 cm^{-1}) are lower than **2a** (1992 cm^{-1}). On the other hand, the Co-C_{CO} or C-O distances exhibit no clear relationship between the oxidation states (Table S1), suggesting the flexibility of structural parameters. Even though evaluation of the oxidation state of the specific metal center is difficult for

heterometallic compounds, we propose the Co^{II} state for **1a** and **2a** because of the used Co^{II} source ($CoCl_2$) for the synthesis of **1a** and retention of the oxidation state in **2a**. Our proposal is in agreement with the significantly higher CO frequency of **2a** (1992 cm^{-1}) than the reported CO frequency (1927 cm^{-1}) of a known Co^{I} tris-carbene complex $[(TIMEN^{xyl})Co(CO)]^+$ ($TIMEN^{xyl}$ = tris[2-(3-arylimidazol-2-ylidene)ethyl]amine).[12] The above-discussed structural flexibility is also found in the comparable Co-C_{CO} distances between the Co^{I} tris-carbene (1.8463(19) Å) and **2a** (1.834(4) Å).

Concerning $[Mo_3S_4Ni]$ clusters, two Ni-CO compounds have been reported as $[(H_2O)_9Mo_3S_4Ni(CO)]^+$ [11b] and $[Cp^*_3Mo_3S_4Ni(CO)]^+$ [11f]. They are in the same $[Mo_3S_4Ni]^{4+}$ state as **2b**, and the Ni-C_{CO} and C-O distances (Table S2) and CO stretching frequencies are comparable among the $[Mo_3S_4Ni]^{4+}$ clusters. The $[Mo_3S_4Ni]^{4+}$ core of **2b** has one more *d*-electron than the $[Mo_3S_4Co]^{4+}$ core of **2a**, and thus, one can anticipate **2b** to facilitate π back-donation to the CO ligand. However, the NiC-O stretching band of **2b** (2039 cm^{-1}) appears at higher frequency than the CoC-O of **2a** (1992 cm^{-1}). Strong orbital interactions of the Ni atom with the $[Mo_3S_4]$ unit rather than π^*(CO) have been discussed previously.[13] Delocalization of Ni *d* electrons in $(dmpe)_3Cl_3Mo_3S_4NiCl$ was suggested by X-ray photoelectron spectroscopy (XPS) measurements and theoretical analysis.[14]

Theoretical Analyses on CO-bound $[Mo_3S_4M]$ Cubes. We have optimized the S = 1/2 and 3/2 spin states of the Co-CO complex **2a**. The S = 1/2 state is the ground state, and the S = 3/2 state lies 19.3 kcal/mol higher in energy. The S = 1/2 ground state of **2a** was experimentally supported by the solution magnetic moment of 1.91μ_B determined by Evans' method. Computed spin densities of the S = 1/2 state confirmed that the unpaired electron is localized mainly at Co (ρCo = 0.82), and the calculated $<S^2>$ value of 0.80 is close to the ideal value (0.75), indicating no spin contamination. In the case of Ni-CO complex **2b**, we have optimized the S = 0 and 1 states. The ground state of **2b** is S = 0, which is in agreement with the diamagnetic nature of **2b** observed from NMR spectroscopy. The optimized S = 1 state is 23.4 kcal/mol higher in energy relative to the ground state. The optimized ground-state structures of **2a** and **2b** reproduced key structural parameters of their crystal structures listed in Tables 1 and S4. The calculated Mo-Mo Mayer bond orders of **2a** and **2b** indicate Mo-Mo bonding, which is larger compared to Co-Mo or Ni-Mo bonding characters (Table S5). Computed Kohn-Sham frontier orbitals of the ground state complexes are shown in Figures S14 and S15. Visual inspections of the Kohn-Sham orbitals in the frontier region suggested that the Co or Ni *d* orbitals are heavily mixed with the Mo-based orbitals. The calculated C-O vibrational frequency of the ground state structures of **2a** and **2b** are 1957 cm^{-1} and 2002 cm^{-1}, respectively. Computed C-O vibrational frequency qualitatively fits with the experimental results (1992 cm^{-1} of **2a** and 2020 cm^{-1} of **2b**) and shows a similar trend. Even though the computed C-O bond distances of the two clusters are almost indistinguishable, the calculated Mayer bond order of C-O in **2b** (2.10) is slightly higher than the corresponding value in cluster **2a** (2.05). Thus, the Ni-CO cluster **2b** is expected to contain a relatively stronger C-O bond than the Co-CO cluster **2a**, as observed in the IR spectra. To obtain quantitative insights into metal-to-CO π back-donation and CO-to-metal σ donation in these clusters, we have performed an energy decomposition analysis (EDA) together with the natural orbitals for chemical valence (NOCV). Numerical data of the EDA-NOCV is summarized in Table 2, and the plots of deformation densities ($\Delta\rho$) are shown in Figure 4. Computed interaction energy (ΔE_{int}) between

Table 1. M-C and C-O bond distances of the calculated and crystal structures of **2a**, **2b**, and **3**, and calculated Mayer bond orders.

	$[Cp^{XL}_3Mo_3S_4Co(CO)]^+$ (**2a**)		
	Bond distances (Å)		Mayer Bond
	DFT [a]	X-ray	Order [a]
Co-C_{CO}	1.75	1.83	1.26
C-O	1.16	0.99	2.05
	$[Cp^{XL}_3Mo_3S_4Ni(CO)]^+$ (**2b**)		
	Bond distances (Å)		Mayer Bond
	DFT [b]	X-ray	Order [b]
Ni-C_{CO}	1.76	1.76	1.11
C-O	1.15	1.15	2.10
	$[Cp^{XL}_3Mo_3S_4Fe(CO)]$ (**3**)		
	Bond distances (Å)		Mayer Bond
	DFT [a]	X-ray	Order [a]
Fe-C_{CO}	1.75	1.77	1.33
C-O	1.17	1.09	1.98

[a] Based on the optimized structure in the S = 1/2 state. [b] Based on the optimized structure in the S = 0 state.

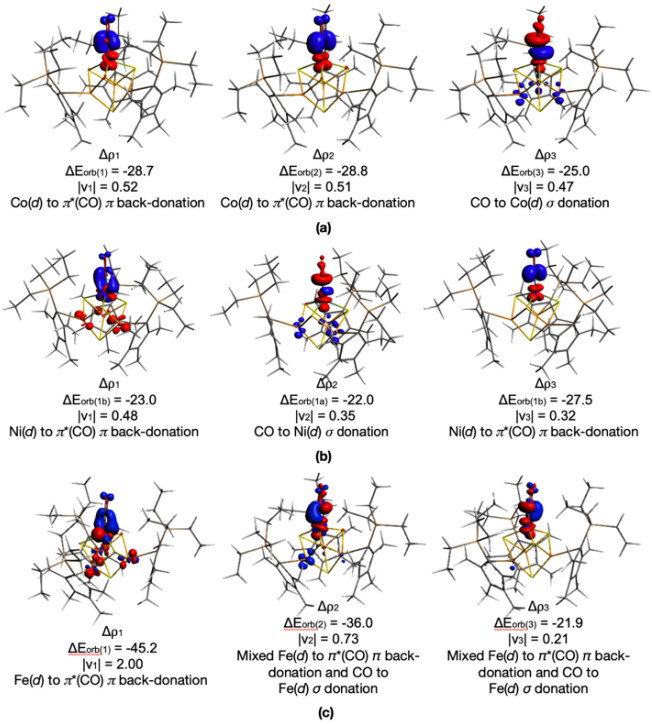

Figure 4. Plots of the deformation densities of clusters **2a** (a), **2b** (b), and **3** (c).

$[Cp^{XL}_3Mo_3S_4Co]$ and CO fragments is –81.5 kcal/mol, while ΔE_{int} between $[Cp^{XL}_3Mo_3S_4Ni]$ and CO fragments is relatively weak (–77.3 kcal/mol). In both systems, electrostatic attraction (ΔE_{elstat}) and orbital interactions (ΔE_{orb}) mainly contribute to overcome the Pauli repulsion (ΔE_{Pauli}). In particular, ΔE_{elstat} and ΔE_{orb} are the dominant components for both complexes, and the latter term is useful in obtaining quantitative insights into interactions between metal and CO.

The ΔE_{orb} of clusters **2a** and **2b** are –93.5 and –79.8 kcal/mol, respectively. Thus, **2a** reveals relatively strong orbital interactions between CO and Co compared to that of between CO and Ni of **2b**. In **2a**, the orb(3) component contributes to the σ donation from CO to Co (–25.0 kcal/mol), while orb(1) and orb(2) contribute to π back-donation from Co to π^*(CO)

Table 2. EDA-NOCV results for **2a**, **2b**, and **3**. The interaction energy (ΔE_{int}) between [$Cp^{XL}_3Mo_3S_4M$] (M = Co, Ni) and CO fragments were separated into Pauli repulsion (ΔE_{Pauli}), electrostatic attraction (ΔE_{elstat}), orbital interactions (ΔE_{orb}), dispersion energy (ΔE_{disp}), and solvation energy (ΔE_{Sol}).

	Calculated energy (kcal/ mol)		
	[$Cp^{XL}_3Mo_3S_4Co$]$^+$ + CO (**2a**)	[$Cp^{XL}_3Mo_3S_4Ni$]$^+$ + CO (**2b**)	[$Cp^{XL}_3Mo_3S_4Fe$]^0 + CO (**3**)
ΔE_{int}	–81.5	–77.3	–101.1
ΔE_{Pauli}	170.5	149.6	196.9
ΔE_{elstat}	–122.0	–115.3	–130.2
ΔE_{orb}	–93.5	–79.8	–125.76
ΔE_{disp}	–10.5	–7.1	–9.26
ΔE_{sol}	–26.0	–24.7	–32.8
$\Delta E_{orb(1)}$	–28.7 (31%) [a]	–23.0 (28%) [a]	–45.2 (36%) [a]
$\Delta E_{orb(2)}$	–28.8 (31%) [a]	–22.0 (26%) [b]	–36.0 (28%) [c]
$\Delta E_{orb(3)}$	–25.0 (27%) [b]	–27.5 (33%) [a]	–21.9 (18%) [c]
$\Delta E_{orb(rest)}$	–10.9 (11%)	–10.8 (13%)	–22.1 (18%)

[a] M(*d*) to π^*(CO) π back-donation. [b] CO to M(*d*) σ donation. [c] Mixed M(*d*) to π^*(CO) π back-donation and CO to M(*d*) σ donation.

(–57.5 kcal/mol in total). Thus, π back-donation is the dominant component in the Co-CO orbital interactions. A qualitatively similar picture can be seen for cluster **2b**, which shows the less significant σ donation from CO to Ni (orb(2), –22.0 kcal/mol) than π back-donation (orb(1) and orb(3), –50.5 kcal/mol in total).

As a result, cluster **2a** has a relatively weak C-O bond that lowers the CO frequency compared to that of **2b**, which is consistent with the experimental results. For the one-electron-reduced Fe analog of **2a** and **2b** ([$Cp^{XL}_3Mo_3S_4Fe(CO)$], **3**), computed S = 1/2 ground state optimized structure has the ΔE_{int} value of –101 kcal/mol, which is stronger compared to **2a** and **2b**. The orb(1) component of **3**contributes to the π back-donation from Fe to CO (–45.2 kcal/mol), which is dominant compared to orb(2) and orb(3) components that hold mixed M(*d*) to π^*(CO) π back-donation and CO to M(*d*) σ donation. The total contribution of the π back-donation to ΔE_{orb} is therefore large in **3** and should result in a strong Fe-C bond as indicated by its Mayer bond order (1.31).

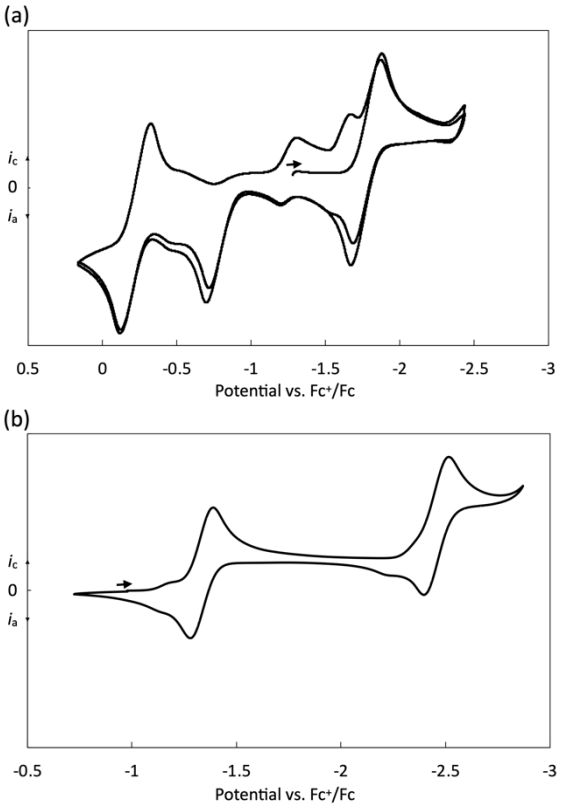

Figure 5. Cyclic voltammograms of [$Cp^{XL}_3Mo_3S_4Fe(CO)$] (**3**) (a) and **2b** (b) in THF. Detailed measurement conditions are described in Supporting Information.

Redox Properties of CO-bound Clusters 2a, 2b, and 3. The strong Fe-CO interaction in **3** was supported experimentally. Our theoretical prediction also suggested sufficient stability of the 1e-oxidized form of **3** ([$Cp^{XL}_3Mo_3S_4Fe(CO)$]$^+$), whose oxidation state corresponds to **2a** and **2b**. However, the synthesis of this compound in a similar manner with **2a** and **2b** was unsuccessful, as mentioned above. Chemical oxidation of [$Cp^{XL}_3Mo_3S_4Fe(CO)$] (**3**) by [Cp_2Fe](PF_6) is a plausible alternative route, but the corresponding reaction mixture showed no signs of metal-bound CO in the IR spectrum. These results, including theoretical analyses, can be explained by an assumption as follows: [$Cp^{XL}_3Mo_3S_4Fe(CO)$]$^+$ is a quasi-stable state under the current reaction conditions, and there are one or more thermodynamically stable species, which have not yet been confirmed. This idea is consistent with the complicated behavior observed in the cyclic voltammogram (CV) of cluster **3** (Figure 5a). A sweep in a region more positive than the rest potential of **3** (*i.e.,* oxidation of [$Cp^{XL}_3Mo_3S_4Fe(CO)$]) displayed an unidentifiable and irreversible oxidation wave at –0.70 V vs. Fc/Fc^+ followed by a reversible redox wave at –0.10 V. Given that clusters **2a** and **2b** exhibited reversible redox couples between [$Cp^{XL}_3Mo_3S_4M(CO)$]$^+$ and [$Cp^{XL}_3Mo_3S_4M(CO)$] (M = Co, Ni) at –0.43 (**2a**) and –1.33 V (**2b**) without other major redox processes (Figures 5b and S10), the unusual behavior of **3** during oxidation suggests structural changes from [$Cp^{XL}_3Mo_3S_4Fe(CO)$]$^+$. Although the predicted *more stable species* remains elusive, it may lead to intriguing reactivity of the CO complex.

The discussed electrochemical measurements of clusters **2a**, **2b** and **3** also revealed well-defined reversible $[Mo_3S_4M]^{3+/2+}$ redox couples observed at –2.62 (for **2a**, [Mo_3S_4Co] cluster), –2.46 (for **2b**, [Mo_3S_4Ni] cluster) and –1.72 (for **3**, [Mo_3S_4Fe] cluster) V vs. Fc/Fc^+, indicating the formation of unrealized $[Mo_3S_4M]^{2+}$ states with CO ligands. In contrast to the theoretical and actual strength of M-CO interactions, the potentials of the $[Mo_3S_4M]^{3+/2+}$ processes did not imply periodic trends, where the values decrease in the order of Fe > Ni > Co. These results should translate into extended stability of the $[Mo_3S_4M]^{3+}$ (*i.e.* [$Cp^{XL}_3Mo_3S_4M(CO)$]^0) state when Co is incorporated. As $[Mo_3S_4Co]^{3+}$ is the sole even electron system among the series

of $[Mo_3S_4M]^{2+}$ clusters (M = Fe, Co, Ni), their electron configurations may affect such disordered redox behaviors.

3. Conclusion

In summary, we have synthesized the Cl-bound $[Mo_3S_4Co]$ and $[Mo_3S_4Ni]$ clusters supported by Cp^{XL} ($C_5Me_4SiEt_3$) ligands. With the known $[Mo_3S_4Fe]$ analog together, we tested the CO-binding behavior of a series of cubic $[Mo_3S_4M]$ clusters (M = Fe, Co, Ni). Removal of the Cl ligand of the $[Mo_3S_4Co]$ and $[Mo_3S_4Ni]$ clusters was attained by simple salt-metathesis, and the resultant cationic species were trapped by CO (1 atm) to provide the cationic CO-bound clusters **2a** and **2b**. An Fe analog of these clusters was not isolable from a similar reaction using the corresponding Cl-bound cluster, whereas the corresponding one-electron reduced form **3** was available via the direct incorporation of the Fe-CO moiety onto the $[Mo_3S_4]$ platform. Theoretical analysis of the isolated CO-bound clusters indicated the significantly stronger M-to-CO back-donation in **3** than in **2a** and **2b**. Even though theoretical analysis also suggested a stable 1e-oxidized form of **3**, $[Cp^{XL}{}_3Mo_3S_4Fe(CO)]^+$, neither synthetic nor electrochemical approaches to detect $[Cp^{XL}{}_3Mo_3S_4Fe(CO)]^+$ were successful, probably due to the presence of more stable unknown species. The identity of this uncharacterized species will be a subject of our future studies, as it is potentially relevant to a novel reactivity of the CO complex. Moreover, the electrochemical analyses on clusters **2a**, **2b**, and **3** demonstrated non-straightforward redox behaviors of the series. These insights may benefit further pursuit of C_1-substrate reductions using the $[Mo_3S_4M]$ clusters and relate the reactivity of the clusters with M-CO interactions.

Supporting Information

Supporting Information is available on http://dx.doi.org/10.1246/bcsj.******. Crystal structures reported in this work were deposited onto Cambridge Crystallographic Database with reference numbers of 2094174 (**1a**), 2094176 (**1b**), 2094175 (**2a**), and 2094177 (**2b**).

Acknowledgement

We thank for the Supercomputing resources at the Research Center for Computational Science at Okazaki (Japan) and the Institute for Chemical Research at Kyoto University (Japan). This study was financially supported by Grant-in-Aids for Scientific Research (19H02733, 20K21207, 21H00021, 20K15295, and 17H06445 for Y.O., 21K20557 and 22K05143 for K.T., and 17H0644 for W. M. C. S.) from the Japanese Ministry of Education, Culture, Sports, Science and Technology (MEXT), CREST grant (JPMJCR21B1 for Y.O.) from JST, the Takeda Science Foundation, the Tatematsu Foundation, the Yazaki Memorial Foundation, International Collaborative Research Program of ICR, Kyoto University (for Y.O. and W. M. C. S.), and Kyoto University Research Fund for Young Scientist (for K.T.).

References

1. For example, see: (a) O. Einsle, D. C. Rees, *Chem. Rev.* **2020**, *120*, 4969. (b) L. C. Seefeldt, Z. Y. Yang, D. A. Lukoyanov, D. F. Harris, D. R. Dean, S. Raugei, B. M. Hoffman, *Chem. Rev.* **2020**, *120*, 5082. (c) A. J. Jasniewski, C. C. Lee, M. W. Ribbe, Y. Hu, *Chem. Rev.* **2020**, *120*, 5107.
2. Y. Kung, C. L. Drennan, *Curr. Opin. Chem. Biol.* **2011**, *15*, 276.
3. K. Tanifuji, Y. Ohki, *Chem. Rev.* **2020**, *120*, 5194.
4. Y. Ohki, K. Uchida, M. Tada, R. E. Cramer, T. Ogura, T. Ohta, *Nat. Commun.* **2018**, *9*, 3200.
5. (a) Y. Ohki, K. Uchida, R. Hara, M. Kachi, M. Fujisawa, M. Tada, Y. Sakai, W. M. C. Sameera, *Chem. Eur. J.* **2018**, *24*, 17138. (b) Y. Ohki, R. Hara, K. Munakata, M. Tada, T. Takayama, Y. Sakai, R. E. Cramer, *Inorg. Chem.* **2019**, *58*, 5230.
6. (a) H. Mori, H. Seino, M. Hidai, Y. Mizobe, *Angew. Chem. Int. Ed.* **2007**, *46*, 5431. (b) M. Ye, N. B. Thompson, A. C. Brown, D. L. M. Suess, *J. Am. Chem. Soc.* **2019**, *141*, 13330. (c) A. Sridharan, A. C. Brown, D. L. M. Suess, *Angew. Chem. Int. Ed.* **2021**, *60*, 12802. (d) A. McSkimming, D. L. M. Suess, *Nat. Chem.* **2021**, *13*, 666.
7. Y. Ohki, K. Munakata, Y. Matsuoka, R. Hara, M. Kachi, K. Uchida, M. Tada, R. E. Cramer, W. M. C. Sameera, T. Takayama, Y. Sakai, S. Kuriyama, Y. Nishibayashi, K. Tanifuji, *Nature* **2022**, doi: 10.1038/s41586-022-04848-1.
8. (a) K. Tanifuji, N. S. Sickerman, C. C. Lee, T. Nagasawa, K. Miyazaki, Y. Ohki, K. Tatsumi, Y. Hu, M. W. Ribbe, *Angew. Chem. Int. Ed.* **2016**, *55*, 15633. (b) N. S. Sickerman, K. Tanifuji, C. C. Lee, Y. Ohki, K. Tatsumi, M. W. Ribbe, Y. Hu, *J. Am. Chem. Soc.* **2017**, *139*, 603. (c) M. T. Stiebritz, C. J. Hiller, N. S. Sickerman, C. C. Lee, K. Tanifuji, Y. Ohki, Y. Hu, *Nat. Catal.* **2018**, *1*, 444.
9. J. Zhou, M. J. Scott, Z. Hu, G. Peng, E. Miünck, R. H. Holm, *J. Am. Chem. Soc.* **1992**, *114*, 10843.
10. (a) M. D. Curtis, U. Riaz, O. J. Curnow, J. W. Kampf, A. L. Rheingold, B. S. Haggerty, *Organometallics* **1995**, *14*, 5337. (b) M. Feliz, R. Llusar, S. Uriel, C. Vicent, E. Coronado, C. J. Gómez-García, *Chem. Eur. J.* **2004**, *10*, 4308. (c) K. Herbst, E. Söderhjelm, E. Nordlander, L. Dahlenburg, M. Brorson, *Inorg. Chim. Acta* **2007**, *360*, 2697. (d) S. Krackl, A. Alberola, R. Llusar, G. Meyer, C. Vicent, *Inorg. Chim. Acta* **2010**, *363*, 4197.
11. (a) T. Shibahara, M. Yamasaki, H. Akashi, T. Katayama, *Inorg. Chem.* **1991**, *30*, 2693. (b) T. Shibahara, S. Mochida, G. Sakane, *Chem. Lett.* **1993**, *22*, 89. (c) K. Herbst, B. Rink, L. Dahlenburg, M. Brorson, *Organometallics* **2001**, *20*, 3655. (d) K. Herbst, M. Monari, M. Brorson, *Inorg. Chem.* **2002**, *41*, 1336. (e) K. Herbst, P. Zanello, M. Corsini, N. D'Amelio, L. Dahlenburg, M. Brorson, *Inorg. Chem.* **2003**, *42*, 974. (f) I. Takei, K. Suzuki, Y. Enta, K. Dohki, T. Suzuki, Y. Mizobe, M. Hidai, *Organometallics* **2003**, *22*, 1790. (g) I. Takei, Y. Wakebe, K. Suzuki, Y. Enta, T. Suzuki, Y. Mizobe, M. Hidai, *Organometallics* **2003**, *22*, 4639. (h) M. Feliz, R. Llusar, S. Uriel, C. Vicent, M. Brorson, K. Herbst, *Polyhedron* **2005**, *24*, 1212. (i) M. N. Sokolov, E. V. Chubarova, R. Hernandez-Molina, M. Clausén, D. Y. Naumov, C. Vicent, R. Llusar, V. P. Fedin, *Eur. J. Inorg. Chem.* **2005**, *3*, 2139. (j) Andrés, M. Feliz, J. Fraxedas, V. Hernández, J. T. López-Navarrete, R. Llusar, G. Sauthier, F. R. Sensato, B. Silvi, C. Bo, J. M. Campanera, *Inorg. Chem.* **2007**, *46*, 2159. (k) R. Hernandez-Molina, J. Gonzalez-Platas, K. A. Kovalenko, M. N. Sokolov, A. V. Virovets, R. Llusar, C. Vicent, *Eur. J. Inorg. Chem.* **2011**, *4*, 683. (l) Y. A. Laricheva, A. L. Gushchin, P. A. Abramov, M. N. Sokolov, *Polyhedron* **2018**, *154*, 202.
12. X. Hu, I. Castro-Rodriguez, K. Meyer, *J. Am. Chem. Soc.* **2004**, *126*, 13464.
13. C. S. Bahn, A. Tan, S. Harris, *Inorg. Chem.* **1998**, *37*, 2770.
14. J. Andrés, M. Feliz, J. Fraxedas, V. Hernández, J. T. López-Navarrete, R. Llusar, G. Sauthier, F. R. Sensato, B.

Silvi, C. Bo, J. M. Campanera, *Inorg. Chem.* **2007**, *46*, 2159.

Graphical Abstract

<Title>
CO Binding onto Heterometals of [Mo_3S_4M] (M = Fe, Co, Ni) Cubes

<Authors' names>
Kazuki Tanifuji, Yuta Sakai, Yuto Matsuoka, Mizuki Tada, W. M. C. Sameera, and Yasuhiro Ohki

<Summary>
Cubic [Mo_3S_4M]-type clusters (M = Co, Ni) with bulky cyclopentadienyl ligands (Cp^{XL}, $C_5Me_4SiEt_3$) were synthesized. CO binding behaviors of the [Mo_3S_4M] cubes (M = Fe, Co, Ni) revealed unexpected instability of $[Cp^{XL}{}_3Mo_3S_4Fe(CO)]^+$ in comparison with $[Cp^{XL}{}_3Mo_3S_4M(CO)]^+$ (M = Co, Ni). Their M-CO interactions were analyzed by DFT calculations.

<Diagram>